Holes and disclinations in hybrid nematic liquid crystal films

Michi Nakata, Darren R. Link, Yoichi Takanishi, Ken Ishikawa, and Hideo Takezoe
Department of Organic and Polymeric Materials, Tokyo Institute of Technology, O-okayama 2-12-1, Meguro-ku, Tokyo 152-8552, Japan
(Received 25 May 2000; revised manuscript received 21 December 2000; published 26 July 2001)

Defect patterns in hybrid nematic liquid crystal films of pentylcyanobiphenyl (5CB) on a glycerol surface were studied with polarized transmission and monochromatic reflected light microscopy. We report that disclinations of apparent topological strength zero, stable pairs of $+1$ and -1 disclinations, and higher strength defects found in these films are stabilized by holes in the liquid crystal film. These holes are produced by a monolayer of surfactant on the glycerol surface. In addition, we describe the topology of the director field in the film during the coalescing of two such holes.

DOI: 10.1103/PhysRevE.64.021709 PACS number(s): 61.30.Jf

I. INTRODUCTION

A hybrid nematic film consists of a thin layer of nematic liquid crystal confined between two different isotropic bounding surfaces. The first hybrid nematic films were prepared on water substrates [1,2], while our system, pentylcyanobiphenyl (5CB) on glycerol, is modeled after that of Lavrentovich and Pergamenshchik as reviewed in [3]. In this system the boundary conditions are planar (tending to align the nematic director **n** parallel to the surface) and homeotropic (tending to align **n** parallel to the film normal) at, respectively, the glycerol and air interfaces. The two-dimensional unit vector field $\mathbf{c}(x,y)$ is then defined as the projection of the average **n** onto the x-y plane as shown in Fig. 1(a). Early studies of hybrid films by Proust *et al.* [2] pointed out the existence of stable holes of a fixed radius playing a role in fixing the orientation of **c**. In particular, they found that holes are topologically equivalent to disclinations of strength $s=+1$ and are accompanied by $s=-1$ disclinations. Point disclinations in two-dimensional systems are rotational defects, whose strength s is defined as the integrated rotation (divided by 2π) of the **c** director over a path encircling the defect. In later studies it was found that as a function of film thickness h a variety of patterns in $\mathbf{c}(x,y)$ can be observed as reviewed by Lavrentovich and Pergamenshchik in Ref. [3]. These patterns include square lattices of disclinations in films less than about 0.5 μm thick [3,4] and stripes in films from around 0.5 μm to 1 μm thick [5]. In films thicker than roughly 1 μm, the patterns become more complex with the appearance of disclinations connected by 2π walls [6] and cellular patterns [3], as well as stable disclination pairs with topological strengths $s=+1$ and $s=-1$, disclinations of apparent topological strength $s=0$, and higher strength disclinations [3,4]. An $s=0$ disclination, as proposed by Lavrentovich and Pergamenshchik, has equal amounts of positive and negative rotation. Previously, it was reported that these structures are governed by the surfacelike terms in the free energy [3]. However, we have found that for the cases of patterns in films thicker than 1 μm, surface elasticity is inadequate to explain experimental observation. In a recent publication, we reported that the disclinations connected by 2π walls and cellular patterns are a consequence of nonuniform film thickness [7]. In the present manuscript we report (i) stable disclination pairs and disclinations of apparent strength $s=0$ are due to holes in the films, (ii) the topology describing the coalescing of two holes, (iii) the accumulation of topological charge on holes leading to the appearance of apparent disclinations of strength larger than $s=1$, and (iv) the origin of the holes is lipid impurities.

II. EXPERIMENT

A. Microscopy

Free surface films were prepared by depositing a dilute solution of 5CB and hexane onto the surface of glycerol and allowing the hexane to evaporate. The resulting films were studied using polarized light transmission microscopy and monochromatic reflected light microscopy. The **c**-director orientation can readily be determined from the polarized light microscopy except for the directional sense (π degeneracy) and the remaining π degeneracy can be removed by noting that **c** is fixed uniquely perpendicular the film edge as explained by Lavrentovich [8] [see Fig. 1(b)]. The existence of holes and the associated thickness variation in the films are readily confirmed by looking at the interference patterns

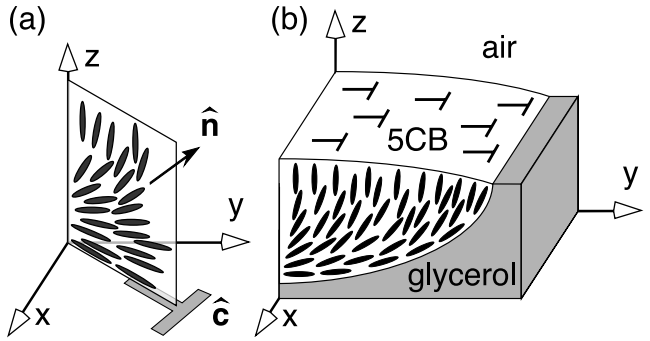

FIG. 1. Molecular orientation in a hybrid nematic film. Molecules tend to align so that the nematic director **n** is parallel and perpendicular to the surface normal at, respectively, the upper and lower surfaces of the film. The **c** director (⊢) is defined as the projection of the average director onto the x-y plane as shown in (a). In a gradient in film thickness $h(x,y)$ the difference in orientation of **n** from the top of the film to the bottom is minimized when **c** is parallel to the gradient, fixing the **c** director normal to the edge of the film as shown in (b).

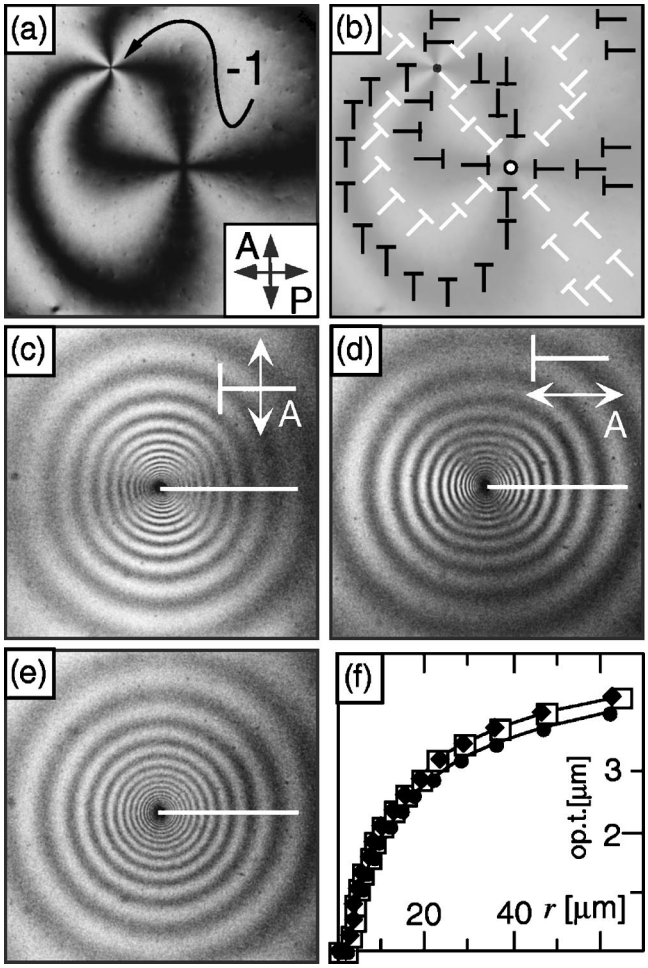

FIG. 2. A stable hole and disclination pair. The transmission image in (a) shows a hole of radius $a=2.2$ μm in a thick $h \sim 3$ μm hybrid nematic film with a -1 disclination located a distance $d=22a$ from the center of the hole. The **c** director (⊢—) is fixed radially at the edge of the hole by the gradient in film thickness as shown in the sketch in (b). The gradient is observed in the monochromatic ($\lambda=532$ nm) reflected light images as shown in (c) and (d) with a single analyzer oriented horizontally and vertically, respectively, as indicated, and in (e) with no polarizers. The plot in (f) shows the optical thickness (op.t) along the horizontal radius (white bar) as determined by counting interference fringes for vertical analyzer (circles), horizontal analyzer (diamonds), and no polarizers (open squares). The horizontal dimension of the photomicrographs is ~ 125 μm.

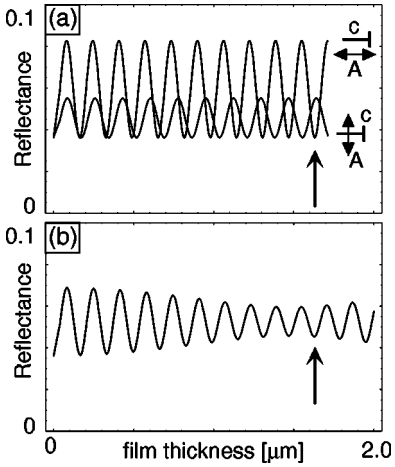

FIG. 3. Calculated reflectance as a function of film thickness for monochromatic light ($\lambda=532$ nm). As shown in (a), the minima in the reflectances calculated for light polarized parallel to **c** (upper curve having $n_1=n_c$) are more closely spaced than the minima for light polarized perpendicular to **c** (lower curve having $n_1=n_0$). When both polarizations are present, the total reflectance is given by half the sum of these curves as is shown in (b). Note that the positions of the minima in (b) are essentially the same as those of the minima for the case of light polarized along **c** as indicated by the arrows pointing to the tenth minimum in both curves.

in the monochromatic reflected light. The interference between the light of wavelength λ reflected from the upper and lower surfaces of a film of thickness h changes from constructive to destructed as the phase difference $(2/\lambda)\int_0^h n(z)\,dz$ changes by π. Although $n(z)$ is a constant equal to n_o throughout the film for light polarized perpendicular to **c**, it varies continuously in the film from top (n_o) to bottom (n_e) for light polarized along **c**. The effect of the birefringence is then to shift the interference patterns for the two polarizations with respect to each other. This effect can be seen in Fig. 2 which shows in 2(a) a photomicrograph of a hole in the film and its companion disclination taken in transmission with crossed polarizers. As sketched in 2(b) the **c**-director field at the edge of the hole is fixed perpendicular to the boundary. This sketch is followed by three photomicrographs of the same hole taken in monochromatic reflected light ($\lambda=532$ nm) with 2(c) an analyzer parallel to the y axis, 2(d) an analyzer parallel to the x axis and, 2(e) no polarizers. The effective optical thickness $\int_0^h n(z)\,dz$ at a given destructive interference fringe is given by $m\lambda/2$, where m is the number of the interference fringe. Figure 2(f) is a plot of the effective optical thickness along the horizontal line from the hole center for each of the photomicrographs shown in 2(c)–2(e).

As the index of refraction perpendicular to **c** is known ($n_0=1.54$), the film thickness profile is directly proportional to the optical thickness for light polarized perpendicular to **c**. The average index of refraction along **c** ($n_c=1.67\pm0.05$) can then be calculated from optical thickness measurements with the analyzer parallel to **c**. Assuming infinitely strong anchoring at the two surfaces and extraordinary index of refraction $n_e=1.73$, and a uniform reorientation of **n** from the top to bottom surface it is calculated that $n_c=(1/h)\int_0^h n(z)\,dz=1.63$, which is within experimental error of the value determined using the film thickness. It is important to note that the contrast in the interference pattern is much higher for light with polarization along **c** than for light polarized perpendicular to **c**, as can be clearly seen in both Figs. 2(c) and 2(d). As a result, when both polarizations are present, Fig. 2(e), the observed interference pattern corresponds to that of light everywhere having a polarization parallel to **c**, i.e., the optical thickness determined from the fringes in both the case of no polarizers and the case of horizontal analyzer are the same as shown in Fig. 2(f).

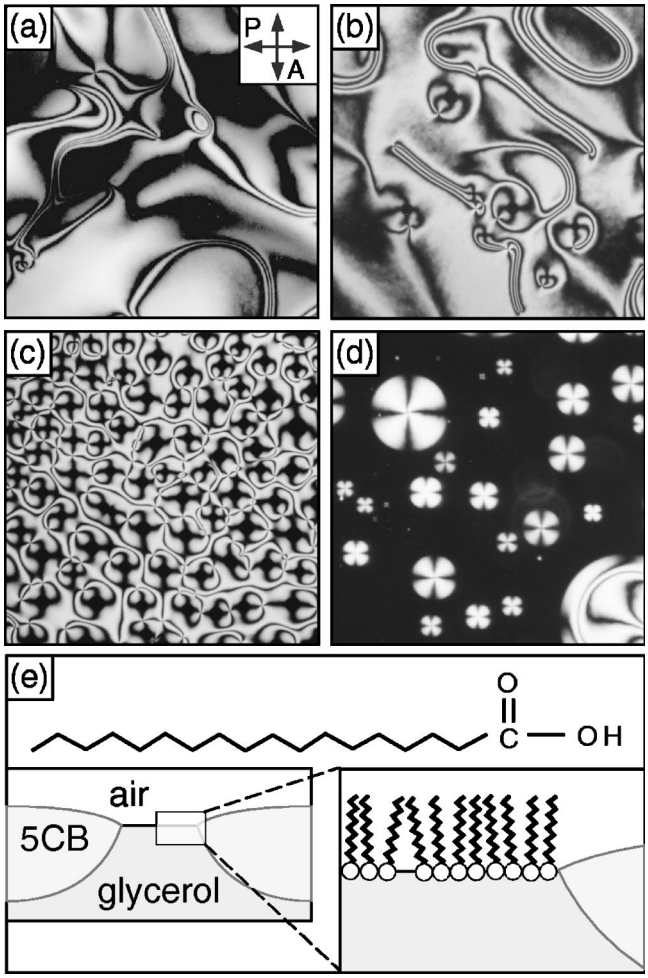

FIG. 4. The effect of surfactant on hybrid nematic films. Shown in (a) is a 2-μm-thick film of 5CB on glycerol. The film is of almost uniform thickness and devoid of any holes. (b) After adding a single drop of hexane containing a small amount of surfactant (~ 1 g/L stearic acid/hexane) and allowing the hexane to evaporate, numerous small holes in the film are observed. These holes become more numerous and larger with the addition of two more drops of surfactant as shown in (c), and in the extreme case of (d) the film breaks up into islands after adding three additional drops to the film of (c). The sketch in (e) shows the molecular structure of stearic acid and a cross-sectional depiction of a hole having a monolayer of stearic acid.

These experimental observations can be understood by considering a thin film of index n_1 between two infinite media, air and glycerol, of indices $n_{air}=1$ and $n_{gly}=1.47$. For normally incident light, the complex reflectivity $r(h)$ is given by

$$r(h)=\frac{n_1(n_{air}-n_{gly})\cos kh - i(n_{gly}-n_1^2)\sin kh}{n_1(n_{air}+n_{gly})\cos kh - i(n_{gly}+n_1^2)\sin kh},$$

where $k=2\pi n_1/\lambda$. The reflectances R, given by $R=|r|^2$, for the cases of $n_1=n_o$ (light polarized perpendicular to **c**) and $n_1=n_c$ (light polarized parallel to **c**) are shown in Fig. 3(a). For unpolarized light the reflectance is given by 1/2 the sum of these curves [see Fig. 3(b)]. As is clear from Fig. 3(b), when both polarizations are present the calculated position of the interference fringes is virtually unchanged from when only the polarization parallel to **c** is present.

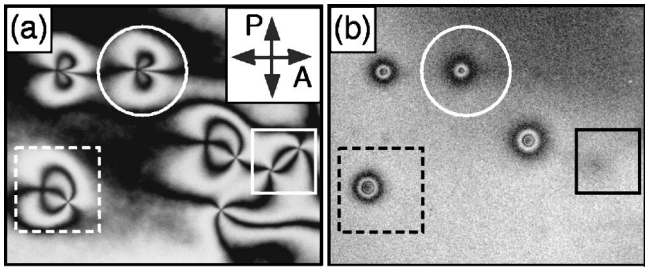

FIG. 5. Defect patterns observed in hybrid nematic films. (a) The **c**-director orientation is determined from the polarized transmission photomicrograph, while (b) information about film thickness is obtained from the corresponding unpolarized monochromatic reflection photomicrograph. Structure 1 (square box with solid border) is a pair of $s=+1$ and $s=-1$ disclinations. These disclinations annihilate after several minutes. Structures 2 (the box with the dashed border) and 3 (circle) consist of a hole and an $s=-1$ disclination. The holes are clearly distinguished from disclinations by the interference fringes in the reflected light ($\lambda=532$ nm) image of (b). In structure 3 the disclination is trapped on the edge of the hole giving the appearance of a disclination of strength $s=0$. The horizontal dimension of the photomicrographs is ~ 100 μm.

From these observations and calculations, we conclude that the interference fringes in the unpolarized monochromatic reflected light patterns correspond to evenly spaced contours in the film thickness of spacing $\Delta h=\lambda/(2n_c)=0.16$ μm (for our experiments $\lambda=532$ nm).

B. Generating holes

A drop of 5CB placed on the surface of glycerol spreads rapidly until the entire surface is covered with a thin film of nematic liquid crystal. Films of various thicknesses can be prepared in this manner and kept stable (without the appearance of holes) for several weeks in a clean environment. If a small amount of hexane is added to such a film, first the hexane dissolves the liquid crystal, making the film isotropic, and then as the hexane evaporates the nematic order returns leaving the film largely unchanged from its original state. Holes in the film are introduced by adding hexane contaminated with a surfactant (in our experiments we use stearic acid). As shown in the photomicrographs of Fig. 4, with an increasing amount of lipid, there is an increasing area of the film that is not covered with liquid crystal. Initially, at low concentrations of lipid, tiny holes in the film are found [Fig. 4(b)], the area of the film occupied by the holes increases with increasing concentration of lipid [Fig. 4(c)]. In the extreme case [Fig. 4(d)] the film breaks up into islands. The films with holes reported in this paper were produced by dissolving both the surfactant, and liquid crystal in hexane and then depositing the hexane mixture on to the surface of glycerol.

Initially when the 5CB, surfactant, and hexane solution is deposited on the surface of the glycerol the mixture is iso-

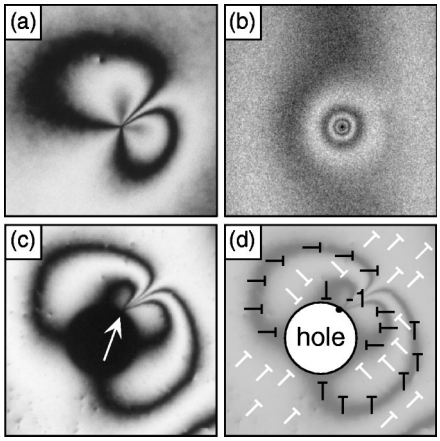

FIG. 6. Apparant strength $s=0$ disclinations. An example of an extremely small hole (less than 1 μm in diameter) with an $s=-1$ disclination trapped on its edge is shown in transmission in (a) and monochromatic reflected light in (b). As all of the brushes close on themselves there is no net rotation of **c** about this structure giving the illusion of an $s=0$ strength disclination. A larger hole (diameter $d=50\,\mu$m) is shown in (c) and sketched in (d). In this case the pointlike disclination [indicated by arrow in (c)] can be easily distinguished on the edge of the hole.

tropic, but as the hexane evaporates there is a first-order transition to a nematic phase exhibiting various patterns [3,7], as well as defects as observed in transmission in Fig. 5(a) and reflection in Fig. 5(b). In Fig. 5 there are three structures that resemble pairs of disclination. The first, structure 1 (the box with the solid border) is a pair of $s=+1$ and -1 disclinations. These disclinations are attracted to each other, moving closer together and annihilating over time as expected. Structure 2 (the box with the dashed border) is in fact a hole accompanied by an $s=-1$ disclination. The structure is stable with both the area of the hole and distance d separating the disclination from the center of the hole remaining constant over time. Structure 3 (circle) also consists of a hole and a -1 disclination, but in this case the -1 disclination is located on the edge of the hole giving the illusion of a disclination of strength $s=0$ [4]. The holes of structures 2 and 3 can clearly be distinguished from $s=+1$ disclinations by the interference fringes observed in the monochromatic reflected light. We have also confirmed that it is possible to make similar defect patterns through the inclusion of silica balls 1 to 5 μm in diameter.

C. Hole-disclination pairs

The hole-disclination pair of structure 2 was previously observed in hybrid nematic films by Proust *et al.* [2]. Transmission and reflection light photomicrographs of this structure in a relatively thick film (3 μm) are shown in Figs. 2(a) and 2(c) with the orientation of the **c** director in the liquid crystal film drawn in the sketch of Fig. 2(b). The radial gradient in film thickness around the edge of the hole requires **c** to point toward the center of the hole, making it equivalent topologically to an $s=+1$ disclination, i.e., **c** is required to rotate through 2π along the border of the hole. At distances far from the center of the hole, a -1 disclination ''sees'' the

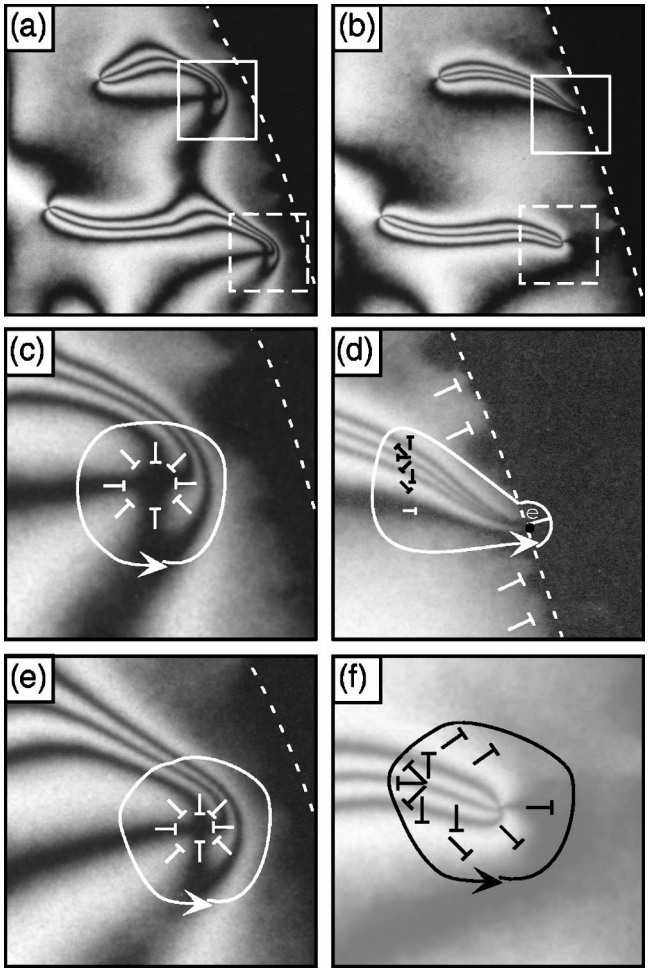

FIG. 7. Disclinations trapped on the film edge. The two holes (solid and dashed boxes) in (a) are moving to the right approaching the film edge (dashed line), and are about to be expelled from the film. After expulsion (b), the topological charge from the upper hole (solid box) is trapped as a disclination on the film edge while the charge from the lower hole (dashed box) forms a $+1$ disclination in the film separated from the film edge (dashed line) and moves back to the left toward the -1 disclination. The regions in the solid boxes in (a) and (b) are enlarged, respectively, in (c) and (d) while those of the dashed boxes are in (e) and (f). The integrated rotation of **c** along a path containing the holes before expulsion (c) and (e) or a defect in the film (f) must be equal to that along a path enclosing the defect trapped on the film edge in (d). This path includes a semicircle of radius ϵ in the region off from the film along which there is no rotation.

hole as a $+1$ disclination and is attracted to it. However, near the edge of the hole, this -1 disclination ''sees'' a boundary with ridge boundary conditions from which it is repelled. Meyer [9] observed similar stable defect structures comprised of a cylindrical air bubble of radius a and a -1 disclination in a hybrid cell. For a two-dimensional vector field the equilibrium position for such a -1 disclination was calculated to be $d=\sqrt{2}a$ [10,11] from the center of the hole. In our system, however, the equilibrium location of the disclinations range from approximately $\sqrt{2}a$ to more than $30a$, significantly further than expected from considerations of

just the boundary conditions. This difference can be qualitatively understood by considering the three-dimensional nature of the film associated with the gradient in film thickness around the hole [8]. Not only does this gradient provide the **c** director with the boundary condition at the edge of the hole, but it also acts as an aligning field on **c** away from the boundary. This aligning field produces the effect of an additional repulsive force on the disclination that is dependent both on film thickness and the radius of the hole. The net result being an increase in the effective hole radius explaining the range in separation distances.

D. Apparent $s=0$ disclinations

Now we turn to discuss the formation and structure of holes with a single -1 disclination trapped on their boundary, structure 3 (circle) in Fig. 5(a). When a surfactant is present, holes can often be observed to spontaneously nucleate in a film of previously uniform **c**-director orientation. As a hole opens the **c** director must rotate in a circle (2π) around its edge to satisfy the boundary conditions. In addition, the **c** director is also required to rotate back through -2π to maintain connectivity with the background orientation, i.e., the topological charge of the film must be conserved. This reverse rotation of the **c** director usually separates from the edge of the hole as an $s=-1$ disclination producing the hole-disclination pair of structure 2 (dashed box). However, occasionally the disclination remains trapped on the edge of the hole producing type-3 structures. The photomicrographs in Figs. 6(a) and 6(b) show an example of a type-3 structure with an exceptionally small hole. Despite its small size (<1 μm) it can still be distinguished as a hole by the interference fringes observed in reflected light. The larger hole in Fig. 6(c) and accompanying schematic 6(d) show the pointlike nature of the -1 disclination on the hole edge.

Previous reports [3,4] indicated that these type-3 structures are disclinations of topological strength $s=0$. These reports speculate that the defect states of both structures 2 and 3 may exist because of a net reduction in the free energy of the system due to the splay canceling mechanism and saddle-splay mechanism. However, experimental observations indicate that $s=0$ disclination are stabilized by holes as opposed to elastic stabilization. From considerations of elastic energy, disclinations on a film edge with rigid boundary conditions should always be repelled from that edge. In this case, however, we speculate that the core energy of the disclinations is reduced when the disclination is on the edge of the film stabilizing it in that position. Our observations are as follows: (i) a hole in the film is always present with these type-3 (and type-2) structures, (ii) these structures never appear in the absence of a surfactant (or an equivalent contaminant), (iii) the disclination can separate from the edge of the hole converting type-3 structures into type-2 structures, and (iv) the 2π rotation of -1 disclination is confined to a narrow 2π wall due to geometrical anchoring [8] as explained in Ref. [7]. Neither strength $s=0$ disclinations nor stable disclination pairs exist in thick hybrid nematic films without holes.

The concept of disclinations trapped on the edge of a film leads to difficulty in the definitions of both the topological strength of the hole and the disclination. The topological strength of a point disclination in two-dimensional systems is typically defined to be the integrated rotation, divided by 2π, of the **c** director along a closed path in the liquid crystal containing the point. However, in the case of disclinations on the film edge such a path does not exist. One way of circumventing this problem is to take the integrated rotation along a path that leaves the film along the arc of a circle of radius ϵ centered on the disclination [see Fig. 7(d)] and attribute no rotation to **c** in regions out of the film. In the limit that ϵ goes

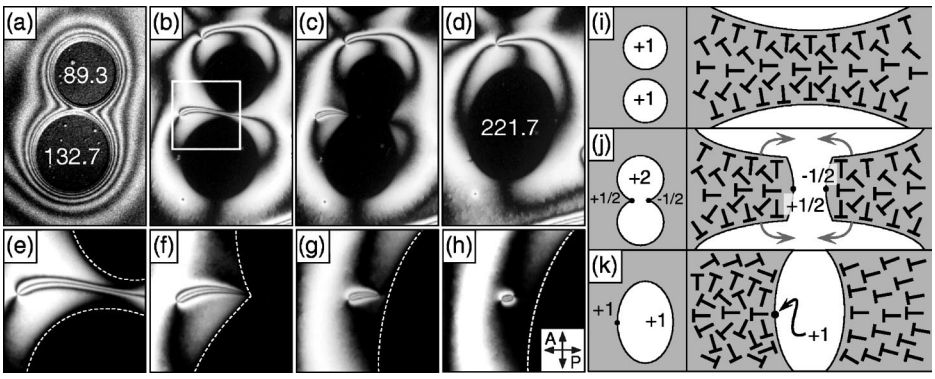

FIG. 8. Coalescing of two holes in a hybrid nematic film. The reflected light image of the two holes (a) clearly shows a thin bridge of liquid crystal. In images (b)–(d) the subsequent time evolution of their coalescing is shown ($\sim$15 s between frames). Note that the total area of the holes is conserved throughout the process. [The area of the holes is given in (a) and (d) in units of μm^2.] Images (e)–(h) show enlargements of the time sequence of the region in the box of (b). In (e) the π change in orientation trapped between the holes can be clearly seen. After the holes coalesce, an $s=+1$ disclination is expelled onto the edge of the film (dotted curve) at the point where the two edges come together (f). This disclination can move off from the edge of the hole and annihilates with one of the -1 disclinations leaving a hole and single -1 disclination as shown in (d). The schematic in (i) shows the **c**-director field (π wall) in the vicinity of the bridge before coalescing. In (j), immediately after coalescing, $+1/2$ and $-1/2$ disclinations are produced at the points of the former bridge. Finally, in (k) the rotation of the edge [see arrows in (j)] as the new hole becomes round increases the strength of the $+1/2$ disclination to $+1$ and unwinds the $-1/2$ disclination completely. The horizontal dimension of the photomicrographs in (a)–(d) is $\sim$800 μm and $\sim$390 μm in (e)–(h).

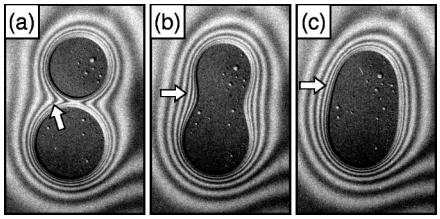

FIG. 9. Monochromatic reflected light images of two holes coalescing. The attractive force between the holes comes from a reduction in surface area as the holes approach and coalesce. This can be visualized by following the change in length of a given contour line through the series. As an aid to the eye, an arrow pointing to the fourth fringe has been added.

to zero, the strength of the disclination is then uniquely defined. This definition for disclinations on the film edge has several advantages. Those being that (i) the strength of the disclination does not change if it moves onto or off from the film edge and (ii) strength s disclinations on the film edge annihilate with strength $-s$ disclinations in the film. Examples of these scenarios are shown in Fig. 7. This figure shows two holes just before they are expelled from a film [solid and dashed boxes in 7(a)] and the resulting disclinations immediately after [respective boxes in 7(b)]. The regions in the boxes with solid borders in 7(a) and 7(b) are, respectively, shown enlarged in 7(c) and 7(d) while the regions with dashed borders are enlarged in 7(e) and 7(f). The holes are each of topological strength $s=+1$ as shown in the schematic of Figs. 7(c) and 7(e). After the lower hole (dashed box) is expelled from the film (the film edge is indicated by the dashed line) the topological charge remains as a $+1$ disclination and moves off from the edge into the film to annihilate with a -1 disclination. In contrast, the topological charge of the upper hole (solid box) remains trapped on the film edge as shown in the schematic of Fig. 7(d). A second -1 disclination approaches this disclination and annihilates with it on the edge (not shown).

E. Coalescing of holes

Although holes (topologically strength $s=+1$) cannot annihilate with disclinations of strength $s=-1$, they can coalesce with each other. Two holes on the verge of coalescing are clearly visible in the reflected light image of Fig. 8(a) with the subsequent evolution shown in the transmission in Figs. 8(b)–8(d). Initially the two holes are each topologically equivalent to two separate $+1$ disclinations, i.e., the integrated rotation of **c** about their perimeters equals 2π and each hole supports a single -1 disclination in the surrounding film. In the bridge region separating the two holes the **c** director is required to rotate through π to match the boundary conditions at the two edges [see Fig. 8(i)]. As the holes approach each other, this π rotation is squeezed continually tighter until the bridge and π-wall break to produce $s=+1/2$ and $-1/2$ disclinations at the points of the former bridge [see Fig. 8(j)]. Conservation of topological strength requires that the integrated rotation of **c** along the border of this new hole to be 4π, as is readily observed, giving it a total topological strength $s=1+1=2$ [see Fig. 8(j)]. Line tension on the edge of the new hole makes the hole round. In that event, the local edge immediately above and below the two half disclinations inevitably rotates through $\pi/2$ with the necessary winding senses shown by arrows in Fig. 8(j). As the **c** director is fixed normal to the edge, this rotation of the local edge adds an additional π rotational to the $s=1/2$ disclination (π rotation) to make it a $+1$ disclination (2π rotation), unwinds the $-1/2$ disclination ($-\pi$ rotation) completely and reduces the topological strength of the new hole to $s=+1$ [see Fig. 8(k)]. The disclination may either remain on the edge of the hole or move off into the film as it attracts one of the -1 disclinations and annihilates with it as is shown in Figs. 8(e)-8(h). The new hole is now stable with a fixed area equal to the sum of the areas of the original two holes. It is topologically equivalent to a $+1$ disclination and it traps a -1 disclination [see Fig. 8(d)].

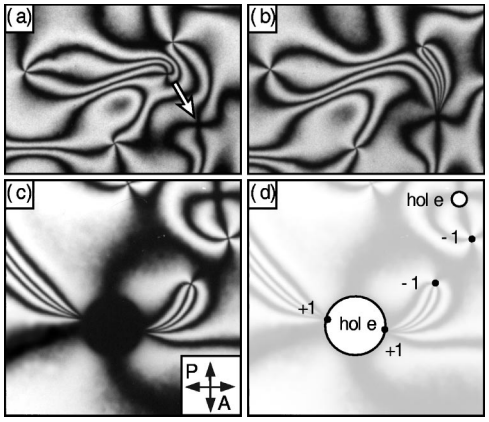

FIG. 10. Apparent high strength disclinations. The photomicrographs in (a) and (b) show two holes before and after coalescing. The topological charge of the smaller hole $(+1)$ is deposited as a $+1$ disclination on the edge of the larger hole. This gives the illusion of a strength $s=+2$ disclination. The arrow in (a) indicates the direction of movement of the smaller hole. Shown in (c) is a structure with 12 black brushes giving the appearance of a disclination of strength $s=+3$. The large hole (diameter $d\sim 40$ μm) makes it easy to distinguish the location of the disclinations on the film edge as sketched in (d). In both (b) and (c) the closest $s=-1$ defect is in the process of annihilating with one of the defects on the hole edge.

The driving force for the coalescing of holes comes from the reduction in the total surface area of the film as the two holes move closer together. An easy way to visualize this is to look at the contours of constant height in the reflection image of Fig. 9. The figure shows a series of reflected light images of two holes as they coalesce. Here we see that the length of a given contour decreases as the two holes move closer together resulting in an attractive force that is dependent on the curvature of the film surface near the film edge. This force increases as the holes move closer together and is strong enough to overcome the repulsive force associated with the π wall squeezed between the two approaching holes.

F. Higher-strength disclinations

One of the interesting consequences of holes being mutually attractive is the production of holes that appear to be

topological disclinations of anomalous strength. Previously it was reported [3,4] that stable disclinations having an arbitrary number of brushes are found to exist in hybrid nematic films. We find that in fact such defects consist of a hole with a number of $s=+1$, and possibly a single $s=-1$, disclinations trapped on its edge. These structures are created when several small holes, each carrying $s=+1$ topological charge, coalesce making a larger hole. The small holes leave their topological charge as disclinations on the edge of the hole after coalescing as shown in Figs. 10(a) and 10(b) before and after such an event. The arrow in (a) shows the direction of movement of the smaller hole as it moves toward the larger hole. If the process happens fast enough [see Figs. 10(c) and 10(d)], a single hole may accumulate several such disclinations before the companion $s=-1$ disclinations of the original holes can approach and annihilate with them. The result is a hole that has a topological charge on its edge that has been deposited by the coalescing of other holes giving the illusion of a higher strength disclination. We never observe disclinations of strength other than $s=\pm 1$ that are not associated with a hole in the film and such holes are never observed in the absence of a surfactant.

III. DISCUSSION

Our interpretation of holes and disclinations in hybrid nematic films is significantly different from that of Proust and *et al.* and Lavrentovich and co-workers. Proust *et al.* have reported the observation of holes of various size opening in hybrid films and that the radius of these holes remains fixed over time. Although they give no explanation of why the holes open they explain that the radius of the holes does not change over time due to a balancing of the surface tensions inside and outside the holes that is achieved independently of the hole radius by a line tension at the hole edge. This line tension is purported to prevent the dewetting of the film [2].

Lavrentovich and co-workers have reported the spontaneous formation of $s=0$ disclinations and higher strength disclinations ($s>+1$) in films of 5CB on glycerol [3,4]. They have argued that the defect state may be energetically preferable than the uniform state owing to the (i) splay canceling mechanism and (ii) saddle-splay mechanism [3,4]. From this rational the spontaneous appearance of $s=0$ disclinations and pairs of $+1$ and -1 disclinations is an indication of the system moving to a lower free energy state. Monte Carlo simulations of Chiccoli *et al.* [12] have also found that in films with a large area to thickness ratio a single strength $s=+1$ disclination can remain in the nematic film after cooling from isotropic. These simulations support the assertion of Lavrentovich and co-workers that it is possible for the free energy of a flat film to decrease upon the generation of disclinations.

We contend, however, that 5CB completely wets the glycerol surface. In contrast to Proust *et al.*, we find that holes in the films only occur when a surfactant is added and the area of these holes is determined by the amount of surfactant. In contrast to Lavrentovich and co-workers, we find that the $s=0$ disclination structure, stable point disclination pairs, and defects of strength $s>1$ do not exist in the absence of holes. It is, in fact, holes in the films that create these structures and the gradient in film thickness at the edge of the holes that gives them their characteristic director orientations. The defect pairs reportedly observed to spontaneously form in flat films [4] are in fact due to micelles of lipid in the glycerol that displace the liquid crystal film when they contact the surface. If the free energy were indeed to be reduced by the introduction of disclinations of strength $s=0$ and $s=\pm 1$ then one would expect the entire film to be filled with them, which is not observed.

The amount of contaminant necessary to produce holes in the films is extremely small. In cases where surfactant is not intentionally added, contaminant can come from skin oils or detergents (found on clothing fibers) as well as a variety of other common sources, resulting in holes. We suspect that this is the case in the observations of both Proust *et al.* and Lavrentovich and co-workers. At the beginning of our investigations, when neither the doping of surfactant nor particular care for contaminant was made, we also observed the spontaneous opening of holes and their associated defects.

IV. CONCLUSION

Contrary to previous claims that surface elasticity stabilizes pairs of $+1$ and -1 disclinations, disclinations of apparent strength zero, and higher strength disclinations, we find that these structures are in fact due to the spontaneous opening of holes in the films. The boundary conditions on these holes make them topologically equivalent to $+1$ disclinations. The holes are stabilized by a monolayer of surfactant that prevents the spreading of the liquid crystal. In films thicker than 1 μm we find that point disclination pairs (having no holes) never form stable structures; rather they attract one another and annihilate. We find no evidence for the spontaneous generation of disclinations in flat uniform hybrid nematic films as proposed by previous experiments [3]. Although our observations indicate that surface elasticity is not important in stabilizing these particular patterns, it may be significant for the stabilization of other patterns such as stripe and lattice patterns found in films thinner than 1 μm. It should be noted that we have confirmed that there are no holes associated with the stable defect lattice patterns, see Fig. 14 of Ref. [3], observed in the thinnest hybrid films.

ACKNOWLEDGMENTS

The authors would like to thank Y. Galerne (IPCMS Strasbourg, France), E. Gorecka (Warsaw University), H. Orihara (Nagoya University), and J.-Z. Xue (Displaytech Inc.) for useful discussions. D.R.L. acknowledges the financial support of the Japanese Society for the Promotion of Science (JSPS).

[1] M. J. Press and A. S. Arrott, Phys. Rev. Lett. **33**, 403 (1974).
[2] J. E. Proust, E. Perez, and L. Terminassian-Saraga, Colloid Polym. Sci. **256**, 666 (1978).
[3] O. D. Lavrentovich and V. M. Pergamenshchik, Int. J. Mod. Phys. B **9**, 2389 (1995).
[4] O. D. Lavrentovich and Y. A. Nastishin, Europhys. Lett. **12**, 135 (1990).
[5] O. D. Lavrentovich and V. M. Pergamenshchik, Mol. Cryst. Liq. Cryst. **179**, 125 (1990).
[6] O. D. Lavrentovich and S. S. Rozhkov, Pis'ma Zh. Éksp. Teor. Fiz. **47**, 210 (1988) [JETP Lett. **47**, 254 (1988)].
[7] D. R. Link, M. Nakata, Y. Takanishi, K. Ishikawa, and H. Takezoe, Phys. Rev. Lett. (to be published).
[8] O. D. Lavrentovich, Phys. Rev. A **46**, R722 (1992).
[9] R. B. Meyer, Mol. Cryst. Liq. Cryst. **16**, 355 (1972).
[10] S. Chandrasekhar, *Liquid Crystals* (Cambridge University Press, Cambridge, 1977).
[11] D. Pettey, T. C. Lubensky and D. R. Link, Liq. Cryst. **25**, 570 (1998).
[12] C. Chiccoli, O. D. Lavrentovich, P. Pasini, and C. Zannoni, Phys. Rev. Lett. **79**, 4401 (1997).